ACS APPLIED MATERIALS & INTERFACES

www.acsami.org

Research Article

# Graphene-Coated PVDF/PAni Fiber Mats and Their Applications in Sensing and Nanogeneration

Md Ashiqur Rahman, Fariha Rubaiya, Nazmul Islam, Karen Lozano, and Ali Ashraf*

Cite This: *ACS Appl. Mater. Interfaces* 2022, 14, 38162−38171

Read Online

ACCESS | Metrics & More | Article Recommendations | Supporting Information

**ABSTRACT:** Forcespinning is a powerful technique to produce fiber systems with suitable properties for a vast array of applications. This study investigates the sensing and energy generation performance of PVDF/PAni fiber mat systems made by the forcespinning method with and without graphene coating. The developed fiber mats were coated with graphene nanoflakes by drop-casting. The graphene-coated nanocomposites show an average output voltage of 75 mV (peak-to-peak), which is 300% higher compared to bare fiber mats, and an output current of 24 mA (peak-to-peak) by gentle finger pressing. Moreover, graphene-coated PVDF/PAni showed a volume conductivity of $1.2 \times 10^{-7}$ S/cm and was investigated as a promising system for temperature (5 times better sensitivity than normal fiber mat), vibration (2 times better voltage generation), and airflow sensing. The graphene-coated composite has been further investigated as a water tide energy harvesting piezoelectric nanogenerator, with the system generating ∼40 mV for a synthetic ocean wave with a flow rate of 30 mL/min. In the future, graphene-coated nanofiber mats can be a solution for low-powered sensors and to harvest blue energy and vibration energy.

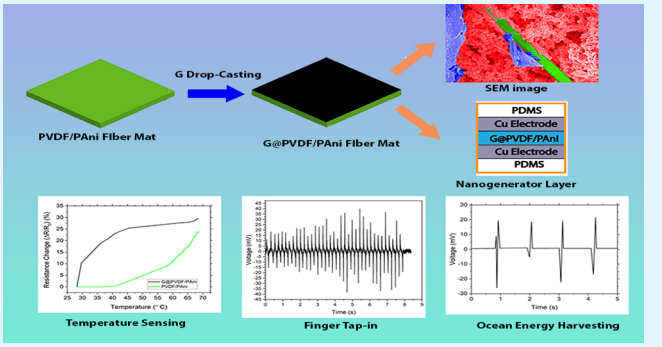


**KEYWORDS:** *forcespinning, conductive polymer, sensing, graphene, nanogeneration*

## INTRODUCTION

Polymers such as poly(vinylidene fluoride) (PVDF) and its copolymers have been widely used due to their piezoelectric properties.[1−5] PVDF is also described as a light, compliant material with high dielectric strength and attractive mechanical properties. PVDF fiber systems have been developed for a variety of applications such as pressure sensing,[6−9] temperature sensing,[10,11] vibration sensing,[12] energy harvesting like nanogeneration,[13−16] and biomedical applications.[17−19] Many attempts have been made in the last few decades to develop nanoscale electrical power generators using a variety of organic and inorganic materials as potential energy harvesters. Personal portable electronic devices, wireless sensing, and implantable biological devices can all be powered by these nanoscale electrical generators. Inorganic materials are brittle and have low formability, which limits their application. Polymeric electrical generators, on the other hand, have excellent formability and are lighter in weight, making them ideal for applications requiring flexibility. Asadnia et al. reported on a single PVDF-based nanofiber sensor fabricated for piezoelectric and nanomechanical characterization as well as to detect oscillatory flow.[20] Reports have also shown that the added presence of a conducting polymer to the PVDF system increases the tensile strength and Young's modulus while decreasing elongation at break.[21] Short conductive strands made of coated multiwall carbon nanotubes (MWCNTs) also aid in the formation of a conductive network in the nanofibers' transverse direction.[22] Merlini et al. demonstrated that PAni-coated electrospun PVDF mats portray interesting properties, including a three-dimensional fiber network structure and electrical conductivity.[23] The piezoelectric performance of a nanogenerator under various external mechanical stresses, such as pressure, tapping, and impact, was demonstrated by an electrospun PAni (polyaniline)/HNT (halloysite nanotube)/PVDF blend nanocomposite,[24] although a low current of as few $\mu$A was obtained. A highly flexible electrospun PVDF/PAni/g-$C_3N_4$ blend nanocomposite (PPBF) nanogenerator (size of ∼5.5 $cm^2$) for piezoelectric energy harvesting with maximum voltage and current output of 30 V and 3.7 $\mu$A, respectively, was successfully developed by Khalifa et al.[25] Yang et al. showed that graphene oxide integration (up to 2%) in PVDF increased the $\beta$-phases of PVDF, and the short-circuit

Received: May 23, 2022
Accepted: August 1, 2022
Published: August 12, 2022

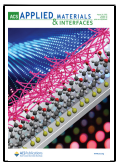

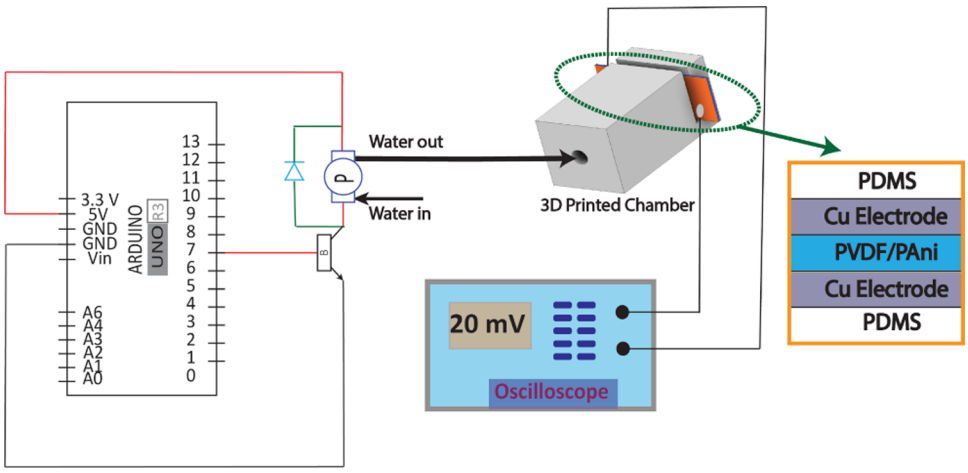


**Figure 1.** Schematic representation of a piezoelectric nanogenerator (PENG) for harvesting water tidal energy (top: components of PENG).

current and open-circuit voltage values were 200 nA and 1.5 V, respectively.[26]

ZnO nanoparticle-PVDF composite thin film demonstrated both enhanced energy generation and motion-sensing capabilities.[27] Composites like SWCNT/a-PVDF are better capacitive systems below a percolation threshold.[28] None of them, however, reported a small PVDF-based fiber sample producing current output in the mA range, which could be revolutionary for blue energy and vibration harvesting nanogenerators.

Forcespinning is a centrifugal-action-based technology for producing nanofibers,[29] with the rotational speed of the spinneret, the design of the collection system, and the shape and size of the needles or nozzles as controlled variables. Drop-casting is a simple technique in which materials are mixed in a suitable solvent and cast by dropping on the target fiber/substrate. For example, Cha et al. used drop-casting to obtain CuO-painted conductive woven textiles for improved energy storage.[30] Vacuum filtration is a procedure in which coating can be done by applying a pressure differential across the fiber/filter. Omi et al. developed a few layers of multiwalled carbon nanotubes (MWNTs) via vacuum filtration for a highly conductive ultrafiltration membrane to get high-quality water free from microorganisms.[31] Dip-coating is a process by which a material is submerged in a coating and dried to make a coating. Highly conductive graphene-coated glass fibers were obtained from the dip-coating method by Fang et al.[32] We used drop-casting for our experiment, as this method is a simple and efficient way for solvent-containing graphene (acetone) to come in contact with the fiber for a suitable period of time for mild etching, leading to the stronger attachment of graphene with fiber. In this work, PVDF/PAni fiber mats were developed utilizing the forcespinning method and subsequently coated with a graphene layer by two different solution drop-casting processes. The effect of graphene on the piezoelectric behavior of the nanocomposites was studied. The result indicated that the enhancement of electrical conductivity was achieved by the graphene nucleation sites within the conductive PVDF/PAni fiber mats. Acetone-based graphene drop-casting showed improved piezoelectric performance and hence the energy harvesting phenomenon like nanogeneration using artificial tidal waves was studied using this nanofiber composite. The electrical properties of spun PVDF/PAni fiber mats and their sensing performance as conductive mats depending on temperature, vibration, and flow were evaluated. The morphology and characterization of graphene-PVDF/PAni composites were also investigated. In the future, we will evaluate different coating techniques with acetone solvent in more detail (vacuum filtration, dip-coating, liquid dispensing using a 3D printer).

## MATERIALS AND METHODS

**Materials.** A KYNAR 741 poly(vinylidene fluoride) (PVDF) powder was obtained from Arkema Inc. Dimethylacetamide (DMA, $CH_3CN(CH_3)_2$) and aniline ($C_6H_5NH_2$) were acquired from Sigma-Aldrich. Acetone ($(CH_3)_2CO$) and ethanol ($C_2H_5OH$) were purchased from Fisher Scientific. Ammonium peroxydisulfate (APS, $(NH_4)_2S_2O_8$) was purchased from Alfa Aesar. Hydrochloric acid (HCl) was bought from Acros Organics.

**Preparation of PVDF/PAni Fiber Mats.** A polymer solution was prepared by adding a 1:1 ratio of DMA and acetone with the PVDF powder. The solution was then fed into the spinneret of a Cyclone system (Fiberio Technology Corporation) and spun at 8000 rpm. The developed nonwoven fiber mats were collected in vertical posts surrounding the spinneret. To coat the PVDF fibers with polyaniline, first, 0.1 M APS was added to a 1 M HCL solution. A PVDF fiber mat was submerged in the solution. Two milliliters of aniline monomer was dropped carefully onto the fiber to cover the whole mat. The whole solution was then covered completely with aluminum foil and left in an orbital shaker for 3 h to facilitate the polymerization process. After turning off the orbital shaker, fiber with the solution was left for 48 h for proper polymerization. Later, the dark green fiber was washed with 0.1 M HCl, distilled water, and ethanol to get rid of any residue. Finally, the fibers were dried overnight at room temperature. This in situ polymerization of polyaniline on PVDF (PVDF/PAni) fiber mat was achieved using a modified procedure described by Singh et al.[33]

**Electrical Characterization.** A rectangular sample size of 20 × 9.5 $mm^2$ with a thickness of 0.4318 mm was sandwiched between two copper electrodes to evaluate the electrical properties of PVDF/PAni nanofibers. The $I-V$ characteristics (volume resistivity) were determined using a Keithley 2450 source meter unit (SMU) and ASTM D4496: Standard Test Method for D-C Resistance or Conductance of Moderately Conductive Materials.

**Temperature Test.** The PVDF-PAni (both coated and uncoated) samples were heated with a hot air gun, and the temperature was measured in real-time with a Fluke RSE 600 infrared (IR) camera. The IR camera and the BK Precision 5491B Multimeter were connected to a computer to obtain temperature and resistance data, respectively.

**Drop-Casting of Graphene on PVDF/PAni.** A homogenizer (Benchmark Scientific-D1000) was used to mix 0.01 g of graphene nanoplatelets (surface area of 750 $m^2/g$, supplied by Sigma-Aldrich)


https://doi.org/10.1021/acsami.2c09045
ACS Appl. Mater. Interfaces 2022, 14, 38162−38171

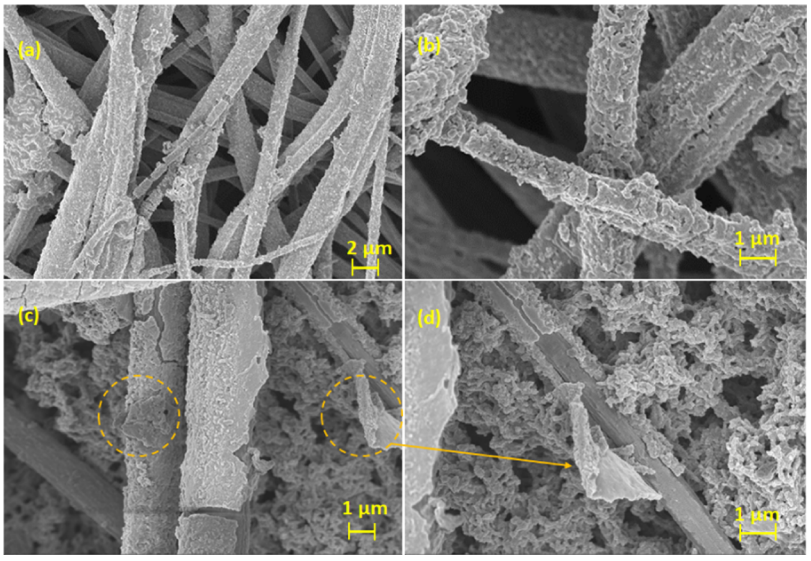


**Figure 2.** SEM images of the PVDF/PAni fiber mat at magnifications of (a) 3000× and (b) 10 000×. SEM images of the G@GPVDF/PAni fiber mat at magnifications of (c) 7710× and (d) 10 000×. Yellow dotted circles represent graphene flakes attached to the fibers.

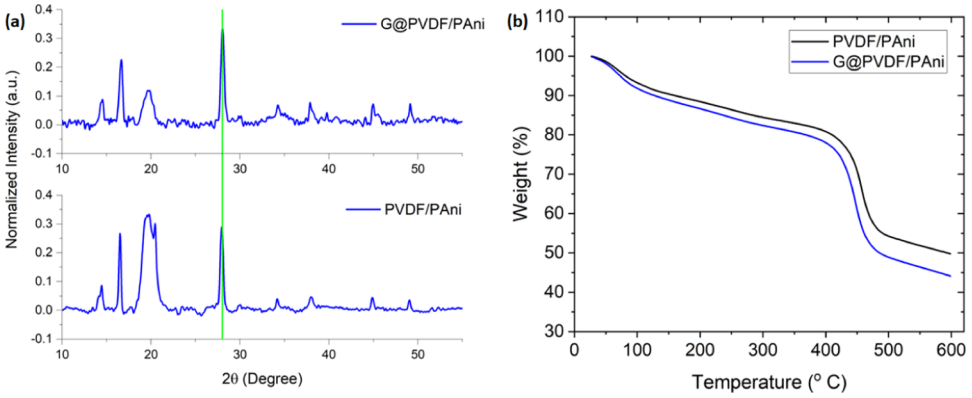


**Figure 3.** (a) X-ray diffraction (XRD) of G@PVDF/PAni and PVDF/PAni fiber mats. (b) Thermogravimetric analysis (TGA) of PVDF/PAni and G@PVDF/PAni.

with 10 mL of isopropyl alcohol and acetone (0.1% w/v solution) for 5 min at different speeds. Two milliliters of volume solution was then drop-cast on two separate PVDF/PAni nanofiber samples (10 × 10 $mm^2$) using a micropipette. The coated sample was kept at ambient conditions for about 1 h to dry out the solvents. Then, the electrodes on both surfaces were made using copper tape, and the PVDF/PAni sample was incorporated with a polydimethylsiloxane (PDMS) (Sylgard 184, Dow Chemicals) as a protective layer. For the rest of this manuscript, the graphene−IPA and graphene−acetone drop-cast samples are labeled as G@PVDF/PAni (IPA) and G@PVDF/PAni, respectively.

**Nanogenerator Using PVDF.** A 3D chamber for the inlet and outlet of the fluid flow to harvest the energy from the water wave (wave created by an Arduino-controlled peristaltic pump switching on and off according to predetermined pulse rate) was constructed. The PVDF/PAni sample (1 × 1 $cm^2$), which was protected on both sides by a PDMS layer, was placed perpendicular to the fluid flow (a small channel was made to avoid the obstruction of the flow). A schematic of the setup is shown in Figure 1.

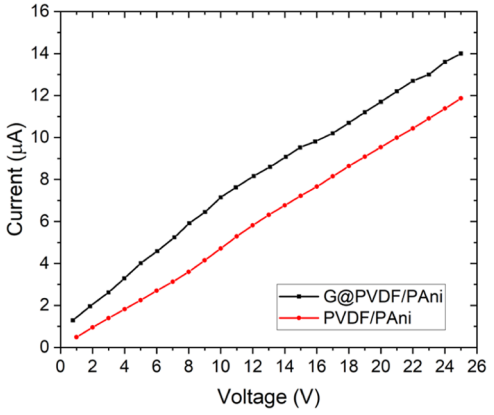


**Figure 4.** Current−voltage ($I$−$V$) characteristics of the conductive PVDF/PAni and G@PVDF/PAni.

## RESULTS AND DISCUSSION

Scanning electron microscopy (SEM) images for the characterization of PVDF/PAni and G@PVDF/PANI are shown in Figure 2. PVDF/PAni fiber nanofibers are characterized by a fibrous structure and a coarse surface in Figure 2a. Better visibility at higher magnification (10 000×) revealed that PAni was uniformly coated on the PVDF nanofibers (Figure 2b). In comparison to the PVDF/PAni nanofiber, a significant amount of PAni densification can be seen in the G@PVDF/PAni SEM image (Figure 2c,d). Additionally, Figure 2c,d shows that graphene flake is well attached to PAni-coated PVDF


https://doi.org/10.1021/acsami.2c09045
ACS Appl. Mater. Interfaces 2022, 14, 38162−38171

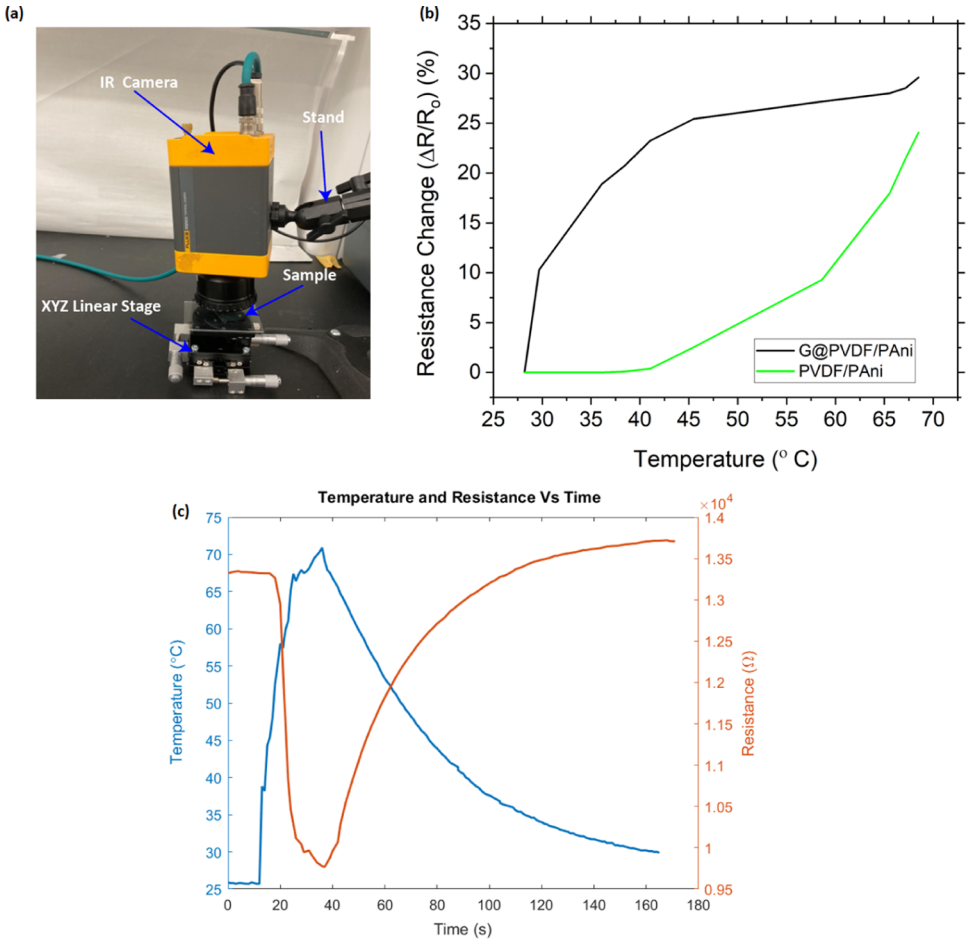


**Figure 5.** (a) Temperature sensing setup having a Fluke RSE 600 thermal camera, close-up lens, and XYZ stage. (b) Temperature change of G@PVDF/PAni and PVDF/PAni with temperature. The sample was heated by a heat gun and resistance was recorded using a BK precision multimeter. (c) Temperature and resistance change with time.

nanofibers (yellow circles). To attach graphene to the fibers, we used acetone to mildly dissolve the PVDF/PAni nanofiber structure. Graphene nanoflakes in acetone then get embedded into the nanofiber upon evaporation of the solvent. Due to this reason, some PAni is removed from the fiber and gets deposited as the densified layer next to the fiber. Figure 3a shows the XRD patterns of PVDF/PAni and G@PVDF/PAni nanofiber composite membranes. PVDF crystallizes primarily in the $\alpha$-phase with distinct peaks at 18.5 and 20.1°. PVDF transforms from $\alpha$-phase to $\beta$-phase as the $\alpha$-phase shows a metastable form, and the formation of the stable form ($\beta$-phase) is accomplished through the rearrangement of the PVDF molecule. The characteristic $\beta$-phase is observed at $2\theta$–20.7° with both G@PVDF/PAni and PVDF/PAni, as shown in Figure 3a. The strong peak at $2\theta$ = 14.0° indicates a high [Cl]/[N] ratio, demonstrating that the PVDF/PAni nanofibers in the composite membranes are highly doped with HCl.[34] G@PVDF/PAni has a characteristic peak in the XRD pattern around $2\theta \sim 27.8°$, indicating that it has a graphitic carbon-based material composition. The peak around $2\theta$–27.8° (green vertical line) is more intense in the G@PVDF/PAni sample compared to the PVDF/PAni fiber mat. This demonstrated that this facile drop-casting process effectively attached graphene to the PVDF/PAni fiber mat. The thermal stability of materials can be determined using thermogravimetric analysis (TGA). We performed TGA in two separate 10 × 10 mm$^2$ samples with a heating rate of 10 °C/min in an $N_2$ gas flow rate of 20 mL/min. RI (100 °C) is associated with water evaporation, RII (100–360 °C) with the decomposition of oxygen-containing groups, and RIII (360–600 °C) with carbon combustion.[35] The onset degradation temperature of the polymer chain for PVDF/PAni is around 420 °C, whereas for G@PVDF/PAni is 410 °C (Figure 3b). This can be attributed to the higher carbon nanomaterial combustion. G@PVDF/PAni loses its mass due to the drop-casting of the graphene–acetone solution, which etches away some of the polymer bonds and hence degrades the graphene-coated sample at a higher rate than the normal PVDF/PAni fiber mat.

Resistivity test using ASTM D4496. The standard test method ASTM D4496 is attributed to DC resistance or conductance of moderately conductive materials. The $I$–$V$ characteristic plot is obtained from Keithley 2450 SMU. The linear relationship between the current and voltage is shown in Figure 4. Volume resistivity (current passing through the body of the fiber mats meaning resistivity across the thickness, whereas surface resistance is the resistance along the surface of a material) determinations are often used in checking the uniformity to detect the impurities that affect the quality of the material. We determined the volume resistivity using eq 1.

$$\rho_v = R_v \frac{A}{t} \tag{1}$$


https://doi.org/10.1021/acsami.2c09045
ACS Appl. Mater. Interfaces 2022, 14, 38162–38171

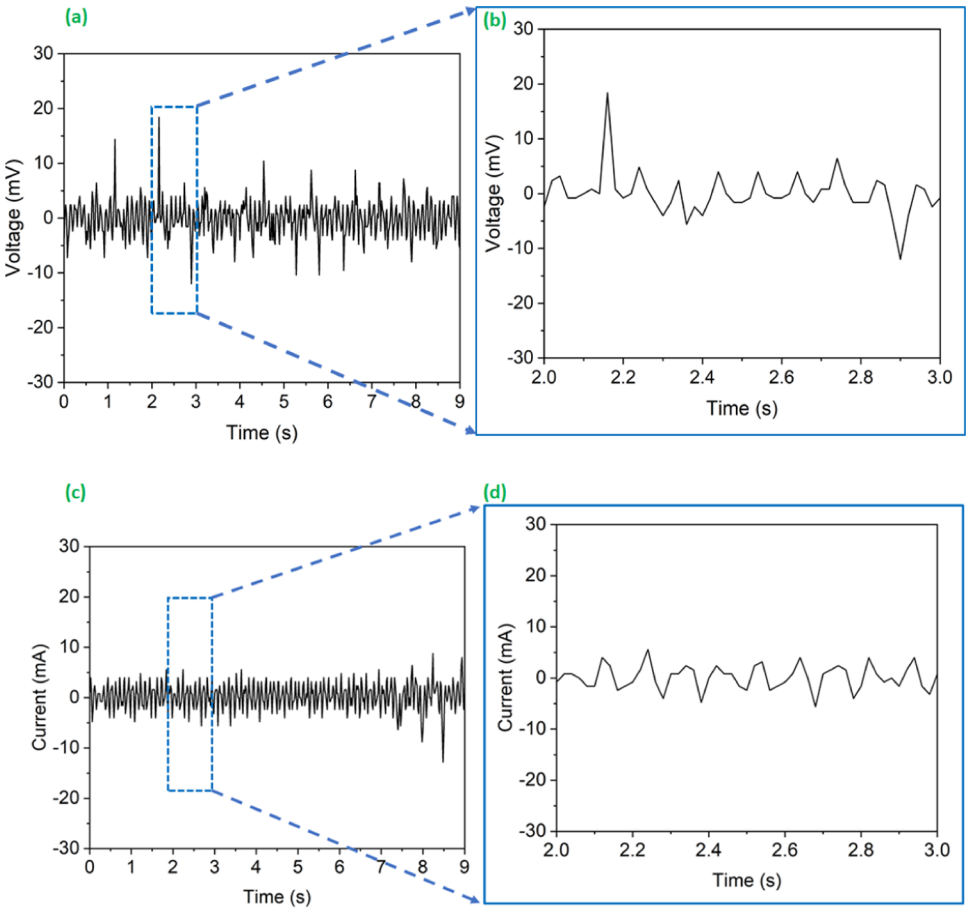


**Figure 6.** (a) Open-circuit voltage ($V_{OC}$) of the PVDF/PAni nanofiber under the finger-pressing condition. (b) Open-circuit voltage ($V_{OC}$) signal during the time from 2 to 3 s. (c) Short-circuit current ($I_{SC}$) of PVDF/PAni PENG under the finger-pressing condition. (d) Short-circuit current ($I_{SC}$) signal during the time from 2 to 3 s.

where $A$ and $t$ are the electrode area and the PVDF/PAni nanofiber mat thickness, respectively, and $R_v$ is the inverse of the slope of the $I-V$ plot. Volume resistivity calculated using the above eq 1 for PDVF/PAni and G@PVDF/PAni is $9.3 \times 10^6$ and $8.31 \times 10^6$ Ω-cm, respectively. Therefore, the volume conductivity (opposite to the volume resistivity) for PVDF/PAni and G@PVDF/PAni is $1.08 \times 10^{-7}$ and $1.2 \times 10^{-7}$ S/cm, respectively.

From the $I-V$ characteristics, the maximum current of the PVDF/PAni fiber mat is around 6.5 μA at 9 V, which is about 4.5 times higher than reported by Chang et al. at 9 V.[36] This verifies the fact that the nanofiber sample can conduct high current.

For temperature sensing, fluorine and hydrogen atoms are located at the two sides of a carbon chain in a polarized PVDF fiber. Therefore, under a stable environment, a negative or positive charge induced perpendicular to the film's surface is constant. However, this equilibrium can be broken if the temperature of the PVDF/PAni film is changed (pyroelectric effect).[2] A Fluke RSE 600 IR camera (Figure 5a) is employed to measure the temperature, and the mean temperature of the sample area is calculated using SmartView R&D and MATLAB software. The resistance of PVDF/PAni decreases when the temperature increases (from room temperature 28 to 70 °C) as more screen charges (surface charges) are released. The resistance changes for G@PVDF/PAni and PVDF/PAni increased to 28 and 22%, respectively, at the maximum temperature of ∼70 °C (Figure 5b,c). Furthermore, the resistance changes for G@PVDF/PAni and PVDF/PAni followed different trends, with G@PVDF/PAni showing higher sensitivity. The combined effects of temperature and airflow were also investigated (Figure S1a,b). The targeted sample area and its corresponding temperature scale are shown in Figure S1c.

In a piezoelectric material, a simple finger tap can induce voltage and current signals. When mechanical stresses in the form of pressure are applied to a piezoelectric film, surface charges are released and move toward the copper electrodes (a positive signal is induced). When the stress is released, charges flow back in the opposite direction, hence producing a negative voltage signal. Compared with that of the pure force spin PVDF/PAni fiber, the conductivity of G@PVDF/PAni was significantly higher due to the atomic interaction between PVDF/PAni and the graphene atom.[37,38] Graphene had a positive effect on the formation of a more conductive network, and it also enhanced the mechanical properties. The structure of the PENG consists of a piece of PVDF/PAni fiber sandwiched between two copper foil electrodes and PDMS. Figures 6a−d and S2a−d present the open-circuit voltage and short-circuit current of PVDF/PAni and G@PVDF/PAni (IPA) nanocomposites, respectively. The signals were achieved under the random finger press. The G@PVDF/PAni (IPA) nanocomposite had better voltage and current signals than the pure PVDF/PAni fiber. Because treating the films with acetone


https://doi.org/10.1021/acsami.2c09045
ACS Appl. Mater. Interfaces 2022, 14, 38162−38171

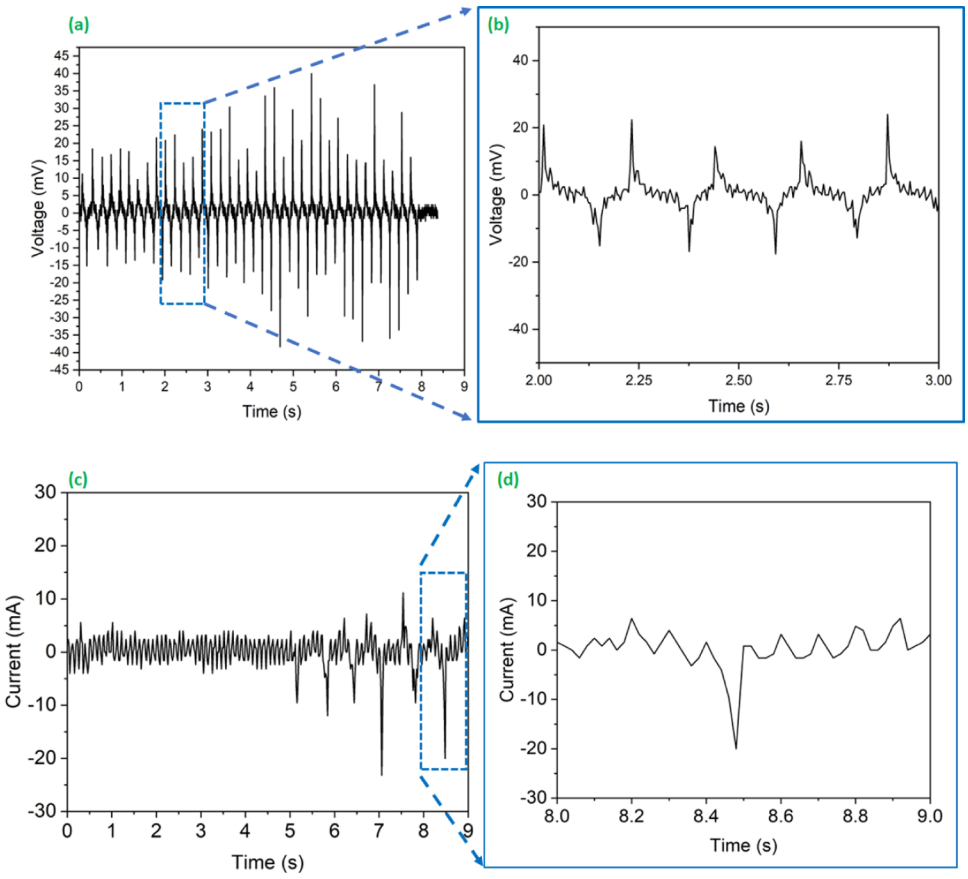


**Figure 7.** (a) Open-circuit voltage ($V_{OC}$) of G@PVDF/PAni under the finger-pressing condition. (b) Open-circuit voltage ($V_{OC}$) generation during the time from 2 to 3 s. (c) Short-circuit current ($I_{SC}$) of G@PVDF/PAni (acetone) under the finger-pressing condition. (d) Short-circuit current ($I_{SC}$) signal for 1 s (enlarged view).

**Table 1. Peristaltic Pump Characteristic Flow Rate with Control Time**

| case | signal on time (ms) | signal off time (ms) | flow rate (mL/min) |
|---|---|---|---|
| 1 | 1000 | 100 | 30 |
| 2 | 1000 | 500 | 24 |

or methanol and the inclusion of graphene increases conductivity,[39] graphene with acetone solution increases the conductivity of the fiber mat. The short-circuit current achieved is 14 mA pk-to-pk compared to 700 nA of the 2% rGO/PVDF sample observed by Yang et al.[26]

Moreover, at the same graphene content, G@PVDF/PAni induced a maximum voltage around 75 mV pk-to-pk (Figure 7a) as compared to 27 mV pk-to-pk by the G@PVDF/PAni (IPA) nanocomposite. Therefore, G@PVDF/PAni prepared using acetone showed better performance than PVDF/PAni and G@PVDF/PAni (IPA) in terms of voltage generation. The G@PVDF/PAni nanocomposite was then employed to a 1 and 2 Hz finger pressing, and the corresponding voltage signals are shown in Figure S3a,b, respectively. The results show the repeatable performance of G@PVDF/PAni under cyclic loading.

Using an Arduino-controlled peristaltic pump, different flow rates with different amplitudes of artificial water waves were created. The corresponding flow rates for different Arduino signal on and off timing are listed in Table 1.

These artificial waves are created to examine nanogeneration performance of the PVDF/PAni sample with and without graphene incorporation. The G@PVDF/PAni sample generates higher peak-to-peak voltages than PVDF/PAni. The maximum voltage generation in G@PVDF/PAni is 40.6 mV peak-to-peak (pk-to-pk), whereas that for PVDF/PAni is only 11.2 mV pk-to-pk (Figure 8a,b). Similarly, for the second case, the maximum voltage generation for G@PVDF/PAni is 43.2 mV, while the PVDF sample produces 28.4 mV (Figure 8c,d). The voltage generation is due to the bending of the sample, which causes the surface charges to be released. As the waves approach with different forces (due to signal pulses provided by Arduino, Figure S4) toward the PVDF/PAni, voltage generation changes over time. This can be very useful to utilize the tidal wave energy using this kind of piezoelectric material.

Vibration is a common phenomenon of back-and-forth motion in opposite directions to an axis. A mini vibrating motor was used to create the fluctuating vibrating motion, and the motor was attached to the PVDF/PAni and G@PVDF/PAni nanofibers (Figure 9a). BK Precision Triple Output Programmable DC Power Supply (Model 9130B) was used to supply the power for the motor (2−4 V). As the voltages increased, the vibration of the motor increased. By recording the sound via a smartphone and analyzing the frequency using Audacity software, vibration magnitude was qualitatively determined from the sound level (Figure S5a). The motor vibration increased with the increasing motor operating voltages for a fixed frequency range (Figure 9b). Vibration motor sound characteristic means that vibration magnitude is in dB (for 2 V supply), and the corresponding sample voltage generation for 0.1 s is also shown in Figure 9c. The induced


https://doi.org/10.1021/acsami.2c09045
ACS Appl. Mater. Interfaces 2022, 14, 38162−38171

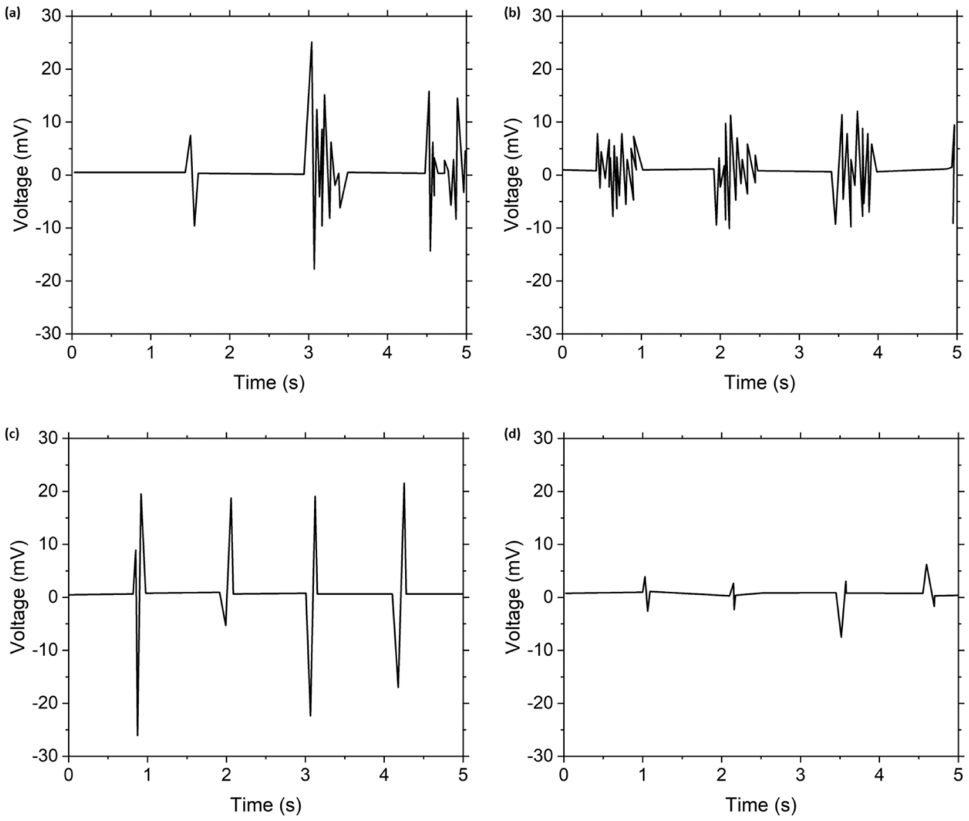


**Figure 8.** Voltage signal for pump switch on 1000 ms and switch off 100 ms of (a) G@PVDF/PAni PENG, (b) PVDF/PAni PENG. Voltage signal for pump switch on 1000 ms and switch off 500 ms of (c) G@PVDF/PAni PENG, (d) PVDF/PAni PENG.

**Table 2. Performance of Different Nanocomposite Nanogenerators Based on PVDF**

| fillers | fabrication | test method | max. voltage output | max. current output | references |
|---|---|---|---|---|---|
| graphene (1.6%) | electrospinning | 3 point bending (1 mm displacement) | 0.5 V | | 40 |
| graphene (0.1%) | electrospinning | finger tap-in | 7.8 V | 4.5 $\mu$A | 41 |
| | electrospinning | 5 g weight dropping | 0.028 V | | 42 |
| graphene oxide (0.4%) | electrospinning | finger tap-in | 1.5 V | | 43 |
| PAni and HNT (halloysite nanotube) | electrospinning | impact loading (14 g weight from 10 cm height) | 7.20 V | 0.75 $\mu$A | 44 |
| graphene and PAni | forcespinning | finger tap-in | 0.075 V | 24 mA | this work |

**Table 3. Performance Differences between PVDF/PAni and G@PVDF/PANI for All Sensing and Nanogeneration Applications**

| | parameters | PVDF/PAni | G@PVDF/PANI | percentage difference |
|---|---|---|---|---|
| temperature sensing | resistance change at 50 (°C) | 5 (%) | 25 (%) | ~400 (%) |
| finger tap-in | max. voltage generation (pk-to-pk) | 18 mV | 75 mV | ~317 (%) |
| | max. current (pk-to-pk) | 14 mA | 24 mA | ~71 (%) |
| nanogeneration using water waves (pump switch on 1000 ms and off 100 ms) | max. voltage generation (pk-to-pk) | 11 mV | 40 mV | ~264 (%) |
| nanogeneration using water waves (pump switch on 1000 ms and off 500 ms) | max. voltage generation (pk-to-pk) | 43 mV | 28 mV | ~54 (%) |
| vibration analysis | voltage generation at vibration motor input voltage 4 V | 26 mV | 12.5 mV | ~108 (%) |

voltages followed a pattern related to motor-generated vibration.

The root mean square voltage ($V_{RMS}$) generated by the sample increased with the motor vibration magnitude level for the PVDF/PAni nanofiber (Figure 9d). Similarly, with the G@PVDF/PAni nanofiber, the voltage generation increased around 2 times that of the PVDF/PAni nanofiber at a similar motor vibration. Voltage signals with time plots are shown in Figure S5b–k. Accordingly, the G@PVDF/PAni sample current for vibration was measured, and the current also increased with the vibration magnitude (Figure S6). A comparison of the piezoelectric performance of different filler-based PVDF nanogenerators is given in Table 2. The maximum voltage and the current of our sample using a simple


https://doi.org/10.1021/acsami.2c09045
ACS Appl. Mater. Interfaces 2022, 14, 38162−38171

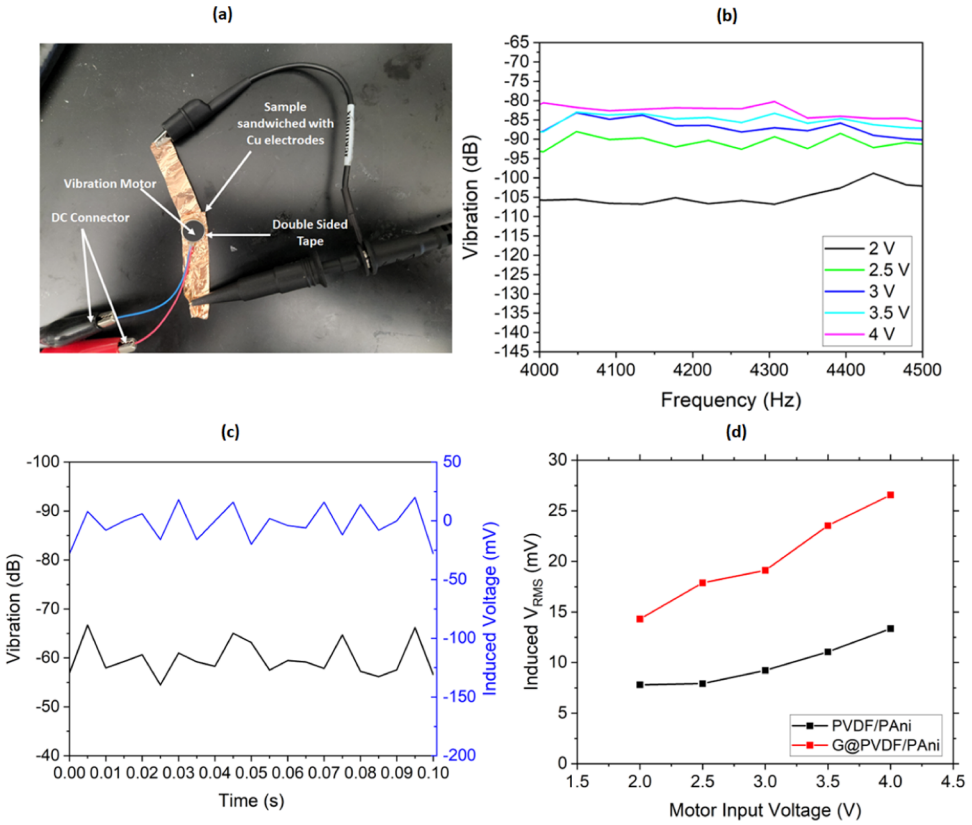


**Figure 9.** (a) Setup image of the sample and vibration motor. (b) Vibration (dB) vs frequency (Hz) plot for different voltages. (c) Vibration motor sound characteristics (for 2 V DC supply) and the corresponding sample voltage generation for 0.1 s. (d) Sample-induced $V_{RMS}$ vs vibration motor operating voltage.

finger tap-in were around 0.075 mV and 24 mA, respectively. Therefore, the network had better electrical conductivity as the current amount was significantly higher (in the mA range) than that reported by others (mostly in $\mu$A to nA range).[40−44]

Graphene added by the drop-casting method increased the conductivity of the PVDF/PAni network. Hence, we obtained 5 times better sensitivity in temperature sensing, ∼4 times better voltage generation in normal finger tap-in, and ∼3.6 times higher voltage generation in nanogenerator using water wave than the normal PVDF/PAni fiber mats (Table 3).

## CONCLUSIONS

Conductive PVDF/PAni nanofiber mats were prepared using the forcespinning method. Mats were coated with a graphene solution using a drop-casting process. The conductivity of coated nanofiber mats was increased, and promising results for the application in temperature, touch, and airflow sensing were reported. The open-circuit voltage generation of the graphene-coated sample using acetone was about 3 times higher than the sample prepared using IPA. G@PVDF/PAni and PVDF/PAni were then investigated to harvest the water tidal energy and vibration energy. It was concluded that the G@PVDF/PAni-based nanogenerator induced 3.6 times and 2 times higher voltages than PVDF/PAni in tidal energy and vibrating energy harvesting methods, respectively. The obtained results pave the way for the potential application of the developed PVDF/PAni nanofiber-based mats as temperature and airflow sensing as well as water tidal energy harvesting nanogenerators.

## ASSOCIATED CONTENT

### Supporting Information

The Supporting Information is available free of charge at https://pubs.acs.org/doi/10.1021/acsami.2c09045.

Temperature and airflow sensing (Figure S1); additional voltage and current signal for finger tap-in (Figure S2); voltage generation in cyclic finger pressing (Figure S3); signal curve for artificial water/tidal wave generation (Figure S4); additional plot for vibration energy harvesting (Figure S5); and current generation due to vibration (Figure S6) (PDF)

## AUTHOR INFORMATION

### Corresponding Author

**Ali Ashraf** − *Department of Mechanical Engineering, University of Texas Rio Grande Valley, Edinburg, Texas 78539, United States;* orcid.org/0000-0002-7437-879X; Email: ali.ashraf.fahad@gmail.com

### Authors

**Md Ashiqur Rahman** − *Department of Mechanical Engineering, University of Texas Rio Grande Valley, Edinburg, Texas 78539, United States;* orcid.org/0000-0001-9510-4635

**Fariha Rubaiya** − *School of Materials Science and Engineering, Georgia Institute of Technology, Atlanta, Georgia 30332, United States*

**Nazmul Islam** − *Department of Electrical and Computer Engineering, University of Texas Rio Grande Valley, Edinburg, Texas 78539, United States*

**Karen Lozano** − *Department of Mechanical Engineering, University of Texas Rio Grande Valley, Edinburg, Texas 78539, United States;* orcid.org/0000-0002-6676-8632

Complete contact information is available at: https://pubs.acs.org/10.1021/acsami.2c09045

### Author Contributions

The manuscript was written through contributions of all authors. All authors have given approval to the final version of the manuscript.

### Funding

Financial support from NSF under grant numbers ERI 2138574 and NSF PREM DMR 2122178 is also gratefully acknowledged.

### Notes

The authors declare no competing financial interest.

## ■ ACKNOWLEDGMENTS

The authors kindly acknowledge the experimental support provided by Dr. Farid Ahmed, Dr. Victoria Padilla, Javier Becerril, Dipannita Ghosh, Dipasree Bhowmick, Md Imrul Kaish, and Mr. Omar Castelan from the University of Texas Rio Grande Valley.

## ■ REFERENCES

(1) Zeng, W.; Tao, X.-M.; Chen, S.; Shang, S.; Chan, H. L. W.; Choy, S. H. Highly durable all-fiber nanogenerator for mechanical energy harvesting. *Energy Environ. Sci.* **2013**, *6*, 2631−2638.
(2) Ueberschlag, P. PVDF piezoelectric polymer. *Sensor Rev.* **2001**, *21*, 118.
(3) Vinogradov, A.; Holloway, F. Electro-mechanical properties of the piezoelectric polymer PVDF. *Ferroelectrics* **1999**, *226*, 169−181.
(4) Broadhurst, M. G.; Davis, G. Physical basis for piezoelectricity in PVDF. *Ferroelectrics* **1984**, *60*, 3−13.
(5) Murayama, N.; Nakamura, K.; Obara, H.; Segawa, M. The strong piezoelectricity in polyvinylidene fluroide (PVDF). *Ultrasonics* **1976**, *14*, 15−24.
(6) Shirinov, A. V.; Schomburg, W. K. Pressure sensor from a PVDF film. *Sens. Actuators, A* **2008**, *142*, 48−55.
(7) Wang, G.; Liu, T.; Sun, X.-C.; Li, P.; Xu, Y.-S.; Hua, J.-G.; Yu, Y.-H.; Li, S.-X.; Dai, Y.-Z.; Song, X.-Y.; et al. Flexible pressure sensor based on PVDF nanofiber. *Sens. Actuators, A* **2018**, *280*, 319−325.
(8) Wang, Y. R.; Zheng, J.; Ren, G.; Zhang, P.; Xu, C. A flexible piezoelectric force sensor based on PVDF fabrics. *Smart Mater. Struct.* **2011**, *20*, No. 045009.
(9) Lee, I.; Sung, H. J. Development of an array of pressure sensors with PVDF film. *Exp. Fluids* **1999**, *26*, 27−35.
(10) Xia, K.; Zhu, Z.; Zhang, H.; Xu, Z. A triboelectric nanogenerator as self-powered temperature sensor based on PVDF and PTFE. *Appl. Phys. A* **2018**, *124*, 1−7.
(11) Pullano, S. A.; Mahbub, I.; Islam, S. K.; Fiorillo, A. S. PVDF sensor stimulated by infrared radiation for temperature monitoring in microfluidic devices. *Sensors* **2017**, *17*, 850.
(12) Pan, X.; Wang, Z.; Cao, Z.; Zhang, S.; He, Y.; Zhang, Y.; Chen, K.; Hu, Y.; Gu, H. A self-powered vibration sensor based on electrospun poly (vinylidene fluoride) nanofibres with enhanced piezoelectric response. *Smart Mater. Struct.* **2016**, *25*, No. 105010.
(13) Briscoe, J.; Dunn, S. Piezoelectric nanogenerators−a review of nanostructured piezoelectric energy harvesters. *Nano Energy* **2015**, *14*, 15−29.
(14) Fan, F. R.; Tang, W.; Wang, Z. L. Flexible nanogenerators for energy harvesting and self-powered electronics. *Adv. Mater.* **2016**, *28*, 4283−4305.
(15) Mahapatra, B.; Patel, K. K.; Patel, P. K. A review on recent advancement in materials for piezoelectric/triboelectric nanogenerators. *Mater. Today: Proc.* **2021**, *46*, 5523−5529.
(16) Lu, L.; Ding, W.; Liu, J.; Yang, B. Flexible PVDF based piezoelectric nanogenerators. *Nano Energy* **2020**, *78*, No. 105251.
(17) Mullaveettil, F. N.; Dauksevicius, R.; Wakjira, Y. Strength and elastic properties of 3D printed PVDF-based parts for lightweight biomedical applications. *J. Mech. Behav. Biomed. Mater.* **2021**, *120*, No. 104603.
(18) Guo, H.-F.; Li, Z.-S.; Dong, S.-W.; Chen, W.-J.; Deng, L.; Wang, Y.-F.; Ying, D.-J. Piezoelectric PU/PVDF electrospun scaffolds for wound healing applications. *Colloids Surf., B* **2012**, *96*, 29−36.
(19) Moran, C. G.; Ballesteros, R. G.; Gomez, E. S. Polivinylidene Difluoride (PVDF) Pressure Sensor for Biomedical Applications, In(ICEEE). *1st International Conference on Electrical and Electronics Engineering, 2004*, IEEE, 2004; pp 473−475.
(20) Sengupta, D.; Kottapalli, A. G. P.; Chen, S. H.; Miao, J. M.; Kwok, C. Y.; Triantafyllou, M. S.; Warkiani, M. E.; Asadnia, M. Characterization of single polyvinylidene fluoride (PVDF) nanofiber for flow sensing applications. *AIP Adv.* **2017**, *7*, No. 105205.
(21) Malmonge, L. F.; Langiano, S. d. C.; Cordeiro, J. M. M.; Mattoso, L. H. C.; Malmonge, J. A. Thermal and mechanical properties of PVDF/PANI blends. *Mater. Res.* **2010**, *13*, 465−470.
(22) Sarvi, A.; Silva, A. B.; Bretas, R. E.; Sundararaj, U. A new approach for conductive network formation in electrospun poly (vinylidene fluoride) nanofibers. *Polym. Int.* **2015**, *64*, 1262−1267.
(23) Merlini, C.; Barra, G. M. d. O.; Ramôa, S. D. A. d. S.; Contri, G.; Almeida, R. d. S.; d'Ávila, M. A.; Soares, B. G. Electrically conductive polyaniline-coated electrospun poly (vinylidene fluoride) mats. *Front. Mater.* **2015**, *2*, 14.
(24) Khalifa, M.; Mahendran, A.; Anandhan, S. Durable, efficient, and flexible piezoelectric nanogenerator from electrospun PANi/HNT/PVDF blend nanocomposite. *Polym. Compos.* **2019**, *40*, 1663−1675.
(25) Khalifa, M.; Anandhan, S. PVDF nanofibers with embedded polyaniline−graphitic carbon nitride nanosheet composites for piezoelectric energy conversion. *ACS Appl. Nano Mater.* **2019**, *2*, 7328−7339.
(26) Yang, J.; Zhang, Y.; Li, Y.; Wang, Z.; Wang, W.; An, Q.; Tong, W. Piezoelectric Nanogenerators Based on Graphene Oxide/PVDF Electrospun Nanofiber with Enhanced Performances by In-Situ Reduction. *Mater. Today Commun.* **2021**, *26*, No. 101629.
(27) Jin, C.; Hao, N.; Xu, Z.; Trase, I.; Nie, Y.; Dong, L.; Closson, A.; Chen, Z.; Zhang, J. X. Flexible piezoelectric nanogenerators using metal-doped ZnO-PVDF films. *Sens. Actuators, A* **2020**, *305*, No. 111912.
(28) Puértolas, J.; García-García, J.; Pascual, F. J.; González-Domínguez, J. M.; Martínez, M.; Ansón-Casaos, A. Dielectric behavior and electrical conductivity of PVDF filled with functionalized single-walled carbon nanotubes. *Compos. Sci. Technol.* **2017**, *152*, 263−274.
(29) Sarkar, K.; Gomez, C.; Zambrano, S.; Ramirez, M.; de Hoyos, E.; Vasquez, H.; Lozano, K. Electrospinning to forcespinning. *Mater. Today* **2010**, *13*, 12−14.
(30) Cha, S. M.; Nagaraju, G.; Sekhar, S. C.; Yu, J. S. A facile drop-casting approach to nanostructured copper oxide-painted conductive woven textile as binder-free electrode for improved energy storage performance in redox-additive electrolyte. *J. Mater. Chem. A* **2017**, *5*, 2224−2234.
(31) Omi, F. R.; Choudhury, M. R.; Anwar, N.; Bakr, A. R.; Rahaman, M. S. Highly conductive ultrafiltration membrane via vacuum filtration assisted layer-by-layer deposition of functionalized carbon nanotubes. *Ind. Eng. Chem. Res.* **2017**, *56*, 8474−8484.
(32) Fang, M.; Xiong, X.; Hao, Y.; Zhang, T.; Wang, H.; Cheng, H.-M.; Zeng, Y. Preparation of highly conductive graphene-coated glass fibers by sol-gel and dip-coating method. *J. Mater. Sci. Technol.* **2019**, *35*, 1989−1995.
(33) Singh, V.; Mohan, S.; Singh, G.; Pandey, P.; Prakash, R. Synthesis and characterization of polyaniline−carboxylated PVC composites: application in development of ammonia sensor. *Sens. Actuators, B* **2008**, *132*, 99−106.

(34) Subramania, A.; Devi, S. L. Polyaniline nanofibers by surfactant-assisted dilute polymerization for supercapacitor applications. *Polym. Adv. Technol.* **2008**, *19*, 725−727.
(35) Farivar, F.; Yap, P. L.; Hassan, K.; Tung, T. T.; Tran, D. N.; Pollard, A. J.; Losic, D. Unlocking thermogravimetric analysis (TGA) in the fight against "Fake graphene" materials. *Carbon* **2021**, *179*, 505−513.
(36) Chang, W.-Y.; Hsu, C.-H. Electromechanical characteristics of Polyvinylidene Fluoride for flexible electronics. *Trans. Can. Soc. Mech. Eng.* **2013**, *37*, 325−333.
(37) Zhang, Y. Y.; Jiang, S.; Yu, Y.; Zeng, Y.; Zhang, G.; Zhang, Q.; He, J. Crystallization behavior and phase-transformation mechanism with the use of graphite nanosheets in poly (vinylidene fluoride) nanocomposites. *J. Appl. Polym. Sci.* **2012**, *125*, E314−E319.
(38) Wu, Y.; Hsu, S. L.; Honeker, C.; Bravet, D. J.; Williams, D. S. The role of surface charge of nucleation agents on the crystallization behavior of poly (vinylidene fluoride). *J. Phys. Chem. B* **2012**, *116*, 7379−7388.
(39) Kinlen, P. J.; Liu, J.; Ding, Y.; Graham, C.; Remsen, E. Emulsion polymerization process for organically soluble and electrically conducting polyaniline. *Macromolecules* **1998**, *31*, 1735−1744.
(40) Abbasipour, M.; Khajavi, R.; Yousefi, A. A.; Yazdanshenas, M. E.; Razaghian, F.; Akbarzadeh, A. Improving piezoelectric and pyroelectric properties of electrospun PVDF nanofibers using nanofillers for energy harvesting application. *Polym. Adv. Technol.* **2019**, *30*, 279−291.
(41) Abolhasani, M. M.; Shirvanimoghaddam, K.; Naebe, M. PVDF/graphene composite nanofibers with enhanced piezoelectric performance for development of robust nanogenerators. *Compos. Sci. Technol.* **2017**, *138*, 49−56.
(42) Gheibi, A.; Bagherzadeh, R.; Merati, A. A.; Latifi, M. Electrical power generation from piezoelectric electrospun nanofibers membranes: electrospinning parameters optimization and effect of membranes thickness on output electrical voltage. *J. Polym. Res.* **2014**, *21*, 1−14.
(43) Zeyrek Ongun, M.; Oguzlar, S.; Doluel, E. C.; Kartal, U.; Yurddaskal, M. Enhancement of piezoelectric energy-harvesting capacity of electrospun $\beta$-PVDF nanogenerators by adding GO and rGO. *J. Mater. Sci.: Mater. Electron.* **2020**, *31*, 1960−1968.
(44) Khalifa, M.; Mahendran, A.; Anandhan, S. Durable, efficient, and flexible piezoelectric nanogenerator from electrospun PANi/HNT/PVDF blend nanocomposite. *Polym. Compos.* **2019**, *40*, 1663−1675.